# Skin Depth Measurements in Varied Metals

Ishaan Aggarwal
Simon Fraser University

## Abstract

This paper presents findings from an investigation into skin depth measurements of various metal conductors, focusing on their electrical and magnetic properties. The study involved subjecting hollow cylindrical conductors to alternating magnetic fields, revealing a shielding effect influenced by conductor dimensions, electrical resistivity, magnetic permeability, and field frequency. Shielding effectiveness was observed to increase exponentially with higher frequencies but remained minimal at lower frequencies. Materials with higher magnetic permeability demonstrated superior field attenuation across frequencies, while lower electrical resistivity was effective at higher frequencies. Notably, introducing a narrow slit along the tube's axis nullified the shielding effect. These insights enhance our understanding of electromagnetic interactions and have practical implications for shielding in diverse electromagnetic environments.

## 1 Introduction

The concept of skin depth was first introduced by the German physicist Horst K. Zahn in 1902 [6], who derived an expression for the attenuation of electromagnetic waves in conductors. He also observed that the skin depth decreases with increasing frequency, and that it depends on the magnetic permeability and the electrical conductivity of the material. Zahn's work was based on the classical theory of electromagnetism, developed by James Clerk Maxwell in the 19th century. However, in the 20th century, quantum mechanics and relativity theory provided new insights into the nature of electromagnetic radiation and its interaction with matter. For example, the skin effect was explained by the scattering of electrons by the electric field of the wave [3], and the anomalous skin effect was discovered, which occurs when the skin depth becomes comparable to the mean free path of the electrons [4]. The skin effect also has implications for the theory of superconductivity, which describes the phenomenon of zero electrical resistance in certain materials at low temperatures. The skin effect is still an active area of research in physics, as it is relevant for many applications in electronics, telecommunications, and material science [5].

Electromagnetic radiation, such as radio waves, microwaves, and light, is composed of oscillating electric and magnetic fields. When these waves encounter a metal conductor, some of them are reflected and some are transmitted. However, the transmitted waves do not propagate freely inside the conductor. They decay exponentially as they penetrate deeper into the material. This is because the alternating magnetic fields induce electric fields and currents in the conductor, known as eddy currents. These eddy currents form closed loops that generate opposing magnetic fields, which reduce the net magnetic flux and current flow inside the conductor. This phenomenon is called the skin effect, and it implies that most of the current is confined to a thin layer near the surface of the conductor. The thickness of this layer is called the skin depth, and it depends on the frequency of the wave and the electrical properties of the material. The skin effect is important for many applications in electronics, telecommunications, and material science, as it affects the resistance, impedance, and power loss of conductors and circuits. Therefore, understanding the skin effect can help design more efficient electronic components and advanced materials. An online tool can be used to calculate the skin depth for different materials and frequencies. For example, aluminum and copper have electrical resistivities of $2.6548 \times 10^{-6} \Omega \cdot \text{cm}$ and $1.678 \times 10^{-6} \Omega \cdot \text{cm}$, respectively. At $10^3$ Hz, the skin depths for aluminum and copper are 2.593 mm and 2.062 mm, respectively. In this experiment, we examine the shielding effects of cylindrical metals in an alternating magnetic field. We measure the magnetic field inside and outside the conducting cylinder and calculate their quotient. We also observe the phase shift of the wave before and after penetrating through the material.

## 2 Theoretical Background

In this section, we will review the basic concepts and equations related to the skin effect, which is the main phenomenon under investigation in this experiment. The skin effect is the tendency for high frequency alternating currents and magnetic fields to penetrate only a thin layer near the surface of a conductor, leaving the interior of the material unaffected. This effect has important implications for the resistance, impedance, and power loss of conductors and circuits, as well as for the design of efficient electronic components and advanced materials.

The skin depth, denoted by $\delta$, is a measure of how far the incident wave can penetrate into the conductor before its amplitude is reduced by a factor of $1/e$. The skin depth

depends on the electrical resistivity, the magnetic permeability, and the angular frequency of the wave. The skin depth can be calculated by the equation

$$\delta = \sqrt{\frac{2\rho}{\mu\omega}} \tag{1}$$

where $\rho$ is the electrical resistivity, $\mu$ is the magnetic permeability, and $\omega$ is the angular frequency of the wave. The skin depth decreases with increasing frequency, meaning that higher frequency waves are more confined to the surface of the conductor.

To determine the amplitude of the alternating magnetic field inside and outside a cylindrical conductor, we need to introduce a dimensionless variable $\nu$, which is given by

$$\nu = Rk_0(1 - i) \tag{2}$$

where $R$ is the radius of the cylinder and $k_0 = \sqrt{\frac{\mu\omega\sigma}{2}}$ is the inverse of the skin-depth length. $\sigma$ is the electrical conductivity of the material, which is the reciprocal of the resistivity. The factor of $(1 - i)$ accounts for the complex nature of the wave propagation in the conductor.

The Bessel functions are special functions that are solutions to a wave equation in cylindrical coordinates. They can be used to describe the wave of the electromagnetic field propagating towards the metal cylinder. The solution for the electric field component in the $\theta$ direction is

$$E_\theta = AJ_1(\nu) + BY_1(\nu) \tag{3}$$

where $J_1$ and $Y_1$ are the Bessel functions of the first and second kind, respectively, and $A$ and $B$ are constants that depend on the boundary conditions. The Bessel functions have a series of zeros and maxima that determine the resonance frequencies of the system.

The magnetic field variation inside the metal can be described by

$$H_z = \frac{k_0(1 + i)}{\mu\omega}(AJ_0(\nu) + BY_0(\nu)) \tag{4}$$

where $J_0$ and $Y_0$ are the Bessel functions of the first and second kind, respectively, and $A$ and $B$ are the same constants as before. The magnetic field inside the conductor is reduced and phase-shifted compared to the magnetic field outside the conductor.

The attenuation coefficient, denoted by $\alpha$, is a measure of how much the incident wave is reduced by the material. It can be calculated by taking the quotient of the magnetic field inside and outside the material. The coefficient is given by

$$\alpha = \frac{4}{\pi\nu^2}\frac{1}{J_2(\nu_1)Y_0(\nu_2) - J_0(\nu_2)Y_2(\nu_1)} \tag{5}$$

where $\nu_i$ is the dimensionless variable inside ($i = 1$) and outside ($i = 2$) the cylinder. The attenuation coefficient is a function of the frequency and the material properties of the conductor. It indicates how effective the material is at shielding the electromagnetic radiation.

# 3 Experimental Methods

The purpose of this experiment was to measure the attenuation coefficient and phase difference of the alternating magnetic field inside different metal pipes using a lock-in amplifier. The experimental setup is shown in Fig. 1.
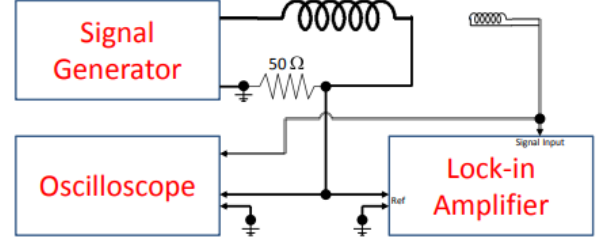


**Figure 3:** Block diagram of Skin-Depth apparatus.

**Figure 1:** Experimental setup for measuring the magnetic field penetration in metal pipes. The function generator, primary and secondary solenoids, lock-in amplifier, and oscilloscope are connected as shown. The slit in some pipes is used to study the eddy currents.

The function generator, Hewlett-Packard 33120A Arbitrary Waveform Generator, was connected to a 50 $\Omega$ resistor and a primary solenoid with 10 turns per centimeter. The primary solenoid produced an alternating magnetic field with a fixed amplitude and a variable frequency ranging from 10 Hz to $10^5$ Hz. The primary solenoid was also connected to the oscilloscope and the lock-in amplifier. The oscilloscope displayed the signal and the lock-in amplifier used it as a reference.

A secondary solenoid or pick-up coil with 200 turns of #38 Formex-insulated copper wire wound around a 3/8 inch diameter glass rod was positioned inside the primary solenoid to capture the generated alternating magnetic field. The secondary solenoid was connected to both the oscilloscope and the lock-in amplifier. The oscilloscope displayed the signal and the lock-in amplifier extracted it from the noise. The specific lock-in amplifier utilized was the Stanford Research System Model SR530 Lock-In Amplifier.

Metal pipes were inserted into the primary solenoid, where the alternating magnetic field tried to penetrate the conductor. The material of these metal pipes included aluminum, copper, stainless steel, and conduit steel. Some of the copper and conduit pipes had a narrow slit along the long axis of the pipes. The slit was used to observe the effect of eddy currents on the magnetic field penetration.

The amplitude and phase of the field inside the metal pipes were obtained from the lock-in amplifier and compared to the field outside the pipes. The ratio of the field amplitude inside and outside the pipes gave the attenuation coefficient at a particular frequency. The difference between the measured phases inside and outside the pipes gave the phase difference between the fields.

The table 1 shows the cylinder wall thickness and the

| Material | Cylinder Wall Thickness | Skin Depth at 10 |
|----------|------------------------|------------------|
| Aluminum | $5.51 \pm 0.01$ mm | $2.09 \pm 0.02$ m |
| Copper | $2.25 \pm 0.01$ mm | $1.64 \pm 0.01$ m |
| Stainless | $3.34 \pm 0.01$ mm | $5.26 \pm 0.1$ m |
| Iron | $3.10 \pm 0.01$ mm | $3.93 \pm 0.03$ m |
| Conduit | $2.45 \pm 0.01$ mm | $3.83 \pm 0.02$ m |

**Table 1:** A table of dimension and skin depth for each cylindrical conductor. The first column is the cylinder wall thickness, and the second column is the skin depth at $10^3$ Hz.



**Figure 2:** Attenuation Coefficient vs. Angular Frequency for different materials, demonstrating frequency-dependent electromagnetic wave penetration.

skin depth for each cylindrical conductor at $10^3$ Hz. The skin depth was computed using Eq. 1, which relates the skin depth to the conductivity, permeability, and frequency of the material. The table reveals that the skin depth is larger than the cylinder wall thickness for all the materials at $10^3$ Hz, meaning that the magnetic field can penetrate through the entire cylinder. However, as the frequency increases, the skin depth decreases, and the magnetic field becomes more attenuated inside the conductor.

# 4   Results

As outlined in the experimental section we tested several materials in the experiment to discover their relative behaviours. Figure 2 illustrates the attenuation coefficient ($\alpha$) as a function of angular frequency ($\omega$) for the materials tested. Utilizing Eq. 5 from our methodology, this plot not only shows how the attenuation coefficient varies with frequency but also provides insights into the frequency-dependent behavior of electromagnetic wave penetration in each material. The depth of penetration, indicated by the attenuation coefficient, varies inversely with frequency, meaning that at higher frequencies, the skin depth decreases, leading to shallower penetration of electromagnetic waves. This phenomenon is crucial for understanding the electromagnetic properties of the materials, as it directly impacts their effectiveness in applications like signal transmission, shielding, and inductive heating. Moreover, the distinct behavior of each material under varying frequencies, as observed in the graph, can be attributed to their intrinsic properties such as electrical conductivity and magnetic permeability. This information is essential for material selection in practical engineering applications, where frequency response is a critical factor.

Comparing the thickness of the cylinders to their skin depth at 103 Hz, we observe a nuanced relationship. The skin depth, defined as the distance required to reduce the wave's amplitude by a factor of $1/e$, is found to be larger than the cylinder's thickness until the wave frequency reaches 103 Hz. As the frequency increases to this point, the skin depth diminishes, allowing for a more substantial interaction between the wave and the cylinder material.

In our analysis of Figure 2, we compare the attenuation coefficients of copper and conduit steel, in both slit and non-sl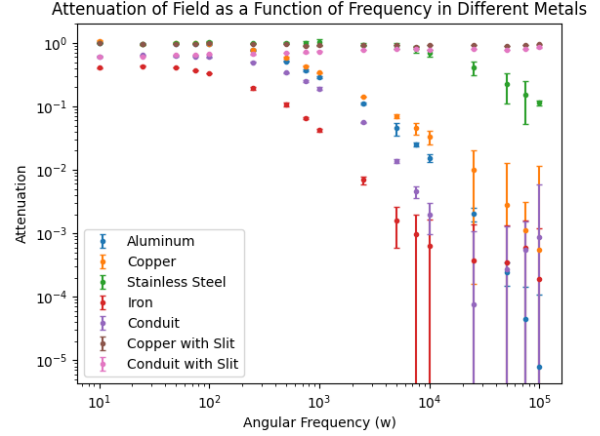it configurations. It becomes evident that cylinders with slits, whether made of copper or conduit steel, exhibit negligible attenuation of the incident magnetic field. Intriguingly, these slitted cylinders behave as if there were no metal inside the solenoid, a phenomenon reminiscent of wave propagation through a slit [3].

Further, our scrutiny of Figure 2 reveals that iron and conduit steel, compared to other materials, begin to attenuate the magnetic field even at lower frequencies. This attribute is due to their higher magnetic permeability as ferromagnetic materials, which tend to redirect magnetic field lines along paths of least resistance. This redirection results in reduced magnetic field intensity due to the materials' propensity for channeling the magnetic field along easier pathways, as referenced in [1]. At higher frequencies, the cylindrical tube walls reach a saturation point, permitting increased magnetic wave penetration. Complementary to this, a study cited in [1] shows that under strong magnetic fields, ferromagnetic materials, such as iron, can become over-saturated, leading to a diminished magnetic shielding effect.

Our observations from Figure 2 classify aluminum, copper, and stainless steel as conductors with low magnetic permeability. These materials show less attenuation of the incident magnetic field, as opposed to their high-permeability counterparts. The differences among these materials are primarily in their dimensions and electrical resistivity. Examining their resistivity, we find that materials with higher resistivity exhibit a less pronounced effect on magnetic field attenuation. This finding underscores the significance of resistivity in determining the extent to which a material influences magnetic field attenuation, shedding light on the electromagnetic behavior of various materials [1].

Figure 3, offers an insightful view into the phase difference as a function of angular frequency for the materials previously examined in the attenuation coefficient study. This graph, derived using Equation 3, is essential for un-
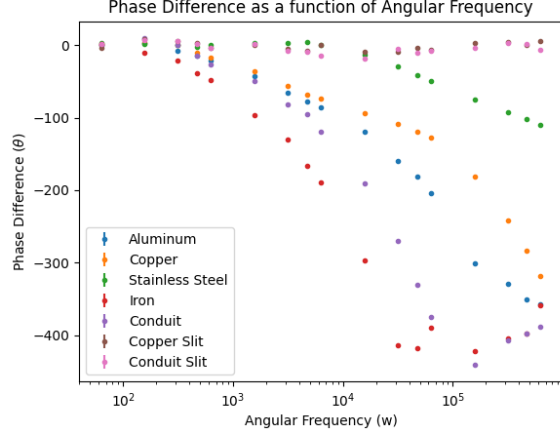
**Figure 3:** Phase vs. Angular Frequency for different materials, demonstrating frequency-dependent electromagnetic wave penetration.



**Figure 4:** Attenuation vs. Angular Frequency for Copper with Curve Fit and Residuals. The graph displays experimental data and a curve fit based on Equation 5. Residuals are shown to assess the accuracy of the fit, illustrating copper's electromagnetic response across various frequencies.

derstanding the phase shift of the magnetic field as it penetrates each material, providing insights into the electromagnetic response of different materials.

The phase difference indicates how the phase of the magnetic field shifts as it penetrates the material. This shift varies significantly across the materials tested, reflecting the unique electromagnetic interactions of each. Materials with higher permeability or conductivity may exhibit more pronounced phase shifts at certain frequencies, indicating their ability to align internal magnetic fields with the external magnetic field. Such characteristics are deeply rooted in the material's intrinsic electromagnetic properties.

Moreover, the graph in Figure 3 is instrumental in elucidating the skin depth phenomenon from a phase perspective. As the frequency increases, the phase shift reveals changes in the penetration depth of electromagnetic waves, especially noticeable in materials with high magnetic permeability, where the phase shift might increase rapidly with frequency.

The resistivity of each material in our study was accurately determined by fitting the experimental data to Equation 5. Our focused analysis on copper, recognized for its exceptional conductive properties, is depicted in Figure 4. This figure showcases the attenuation curve for copper alongside the curve obtained from the model fit. The derived value of $1.69 \times 10^{-8} \pm 0.04\,\Omega \cdot m$ is in close agreement with the known resistive properties of copper. This precise estimation underscores the effectiveness of our model in capturing the electrical resistance characteristics of copper.

Figure 4 not only displays the attenuation curve but also incorporates the residuals from the fitting process. These residuals, which are the differences between the experimental data points and the fitted curve, were found to be minimal. The small magnitude of these residuals is indicative of the accuracy of the fitting process and the suit-
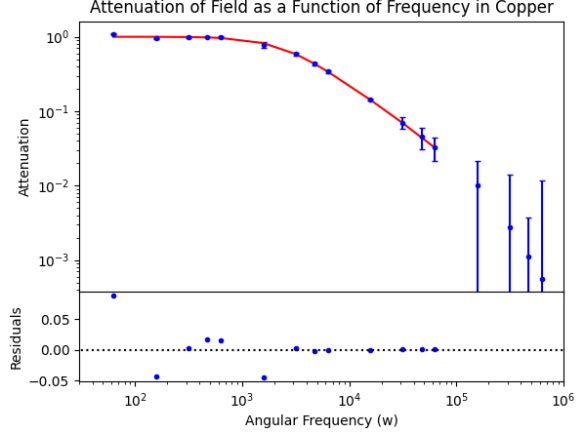
ability of our model in representing the empirical data.

Table 2 compares the resistivity values obtained from our model fitting with conventional DC resistivity measurements[2]. This comparison validates the accuracy of our experimental approach.

**Table 2:** Comparison of resistivity values from conventional DC measurements and model fitting.

| Material | Resistivity ($\Omega \cdot m$) | Permeability (H/m) | Fitted Resisti |
|---|---|---|---|
| Aluminum | $2.82 \times 10^{-8}$ | $\sim 1$ | $2.75 \pm 0.05$ |
| Copper | $1.67 \times 10^{-8}$ | $\sim 1$ | $1.69 \pm 0.04$ |
| Stainless | $6.90 \times 10^{-7}$ | $\sim 1$ | $1.74 \pm 0.1$ |
| Iron | $1.00 \times 10^{-7}$ | $\sim 100$ | $9.87 \pm 0.03$ |
| Conduit | $\sim 9 \times 10^{-8}$ | $\sim 100$ | $1.08 \pm 0.8$ |

The agreement between conventional and experimentally determined resistivity values confirms the effectiveness of our experimental approach. The discrepancy observed in stainless steel is attributed to variations in material properties due to different grades and manufacturing processes.

## 5   Conclusion

In the course of this research, we conducted a series of skin depth measurements on various metal conductors, with a particular emphasis on their electrical and magnetic properties. Our experimental setup involved subjecting hollow cylindrical conductors to an alternating magnetic field, revealing an intriguing shielding phenomenon confined within the cylinder. Noteworthy among our findings were the numerous factors influencing the strength of this shielding effect, including the conductor's dimensions, electrical resistivity, magnetic permeability, and the

frequency of the applied magnetic field.

A significant observation emerged regarding the relationship between shielding effectiveness and the frequency of the magnetic field. As the frequency increased, a noticeable enhancement in shielding effectiveness was observed, characterized by a distinct negative exponential growth pattern. Conversely, at lower frequencies, the shielding effect was, to a practical extent, negligible.

Furthermore, our experiments provided valuable insights into the roles of magnetic permeability and electrical resistivity. Materials with higher magnetic permeability consistently demonstrated a superior ability to attenuate the incident magnetic field, outperforming materials with lower magnetic permeability across a wide frequency spectrum. Additionally, lower electrical resistivity proved to be particularly effective in mitigating the impact of the incident magnetic field at higher frequencies. However, at lower frequencies, resistivity exerted minimal influence on the shielding effect.

One intriguing revelation from our study was the introduction of a narrow slit along the axis of the cylindrical tube. This seemingly minor alteration had a profound impact, effectively nullifying the shielding effect, rendering it akin to the absence of any metal tube within.

In summary, our comprehensive investigation into skin depth measurements and shielding phenomena deepened our understanding of the intricate interactions between electromagnetic fields and conductive materials. These insights offer valuable perspectives on the practical applications and limitations of shielding mechanisms in various electromagnetic environments.

# References

[1] B. D. Cullity and C. D. Graham. *Introduction to Magnetic Materials*. Wiley-IEEE Press, 2008.

[2] Anne Marie Helmenstine. Table of electrical resistivity and conductivity. ThoughtCo, 2019. Available online: `https://www.thoughtco.com/table-of-electrical-resistivity-conductivity-608499`.

[3] Wolfgang Pauli. On the classical radiation of accelerated electrons. *Physical Review*, 63(5-6):209–231, 1943.

[4] Arnold Sommerfeld. über die ausbreitung der wellen in der drahtlosen telegraphie. *Annalen der Physik*, 333(4):665–736, 1909.

[5] E V Stenson, J Horn-Stanja, M R Stoneking, and T Sunn Pedersen. Debye length and plasma skin depth: two length scales of interest in the creation and diagnosis of laboratory pair plasmas. *Journal of Plasma Physics*, 83(1):595830106, 2017.

[6] Horst K Zahn. über die dämpfung der elektromagnetischen wellen an metallen. *Annalen der Physik*, 313(11):833–864, 1902.